

AD-A269 895

22

PL-TR-92-2249



# PERFORMANCE PREDICTIONS FOR THE MSX SPIRIT III INTERFEROMETER SPECTROMETER

Alexander S. Zachor

Boston College  
Institute for Space Research  
140 Commonwealth Avenue  
Chestnut Hill, MA 02167

31 March 1992

DTIC  
ELECTE  
SEP 14 1993  
S B D

Scientific Report No. 1

Approved for public release; distribution unlimited



**PHILLIPS LABORATORY**  
Directorate of Geophysics  
**AIR FORCE SYSTEMS COMMAND**  
**HANSCOM AIR FORCE BASE, MA 01731-5000**

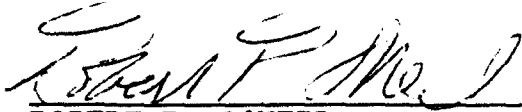
93 9 14 053

93-21346



34 pages

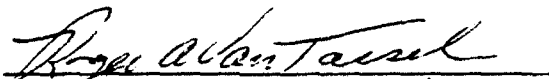
"This technical report has been reviewed and is approved for publication"



ROBERT R. O'NEIL  
Contract Manager  
Simulation Branch



WILLIAM A.M. BLUMBERG, Chief  
Simulation Branch



ROGER A. VAN TASSEL, Director  
Optical Environment Division

This report has been reviewed by the ESC Public Affairs office (PA) and is releasable to the National Technical Information Service (NTIS).

Qualified requesters may obtain additional copies from the Defense Technical Information Center. All others should apply to the National Technical Information Service.

If your address has changed, or if you wish to be removed from the mailing list, or if the address is no longer employed by your organization, please notify PL/TSI, Hanscom AFB, MA 01731-5000. This will assist us in maintaining a current mailing list.

Do not return copies of this report unless contractual obligations or notices on a specific document requires that it be returned.

# REPORT DOCUMENTATION PAGE

Form approved  
OMB No 0704 0188

Public reporting burden for this collection of information is estimated to average 1 hour per response, including the time for reviewing instructions, searching existing data sources, gathering and maintaining the data needed, and completing and reviewing the collection of information. Send comments regarding this burden estimate or any other aspect of this collection of information, including suggestions for reducing this burden, to Washington Headquarters Services, Directorate for Information Operations and Reports, 1215 Jefferson Davis Highway, Suite 1204, Arlington, VA 22202-4302, and to the Office of Management and Budget, Paperwork Reduction Project (0704-0188), Washington, DC 20503.

<b>1. AGENCY USE ONLY (Leave blank)</b>		<b>2. REPORT DATE</b> 31 March 1992	<b>3. REPORT TYPE AND DATES COVERED</b> Scientific No. 1	
<b>4. TITLE AND SUBTITLE</b> Performance Predictions for the MSX SPIRIT III Interferometer Spectrometer			<b>5. FUNDING NUMBERS</b> PE 63214C PR S321 TA06 WUAN Contract F19628-91-K-0001	
<b>6. AUTHOR(S)</b> Alexander S. Zachor				
<b>7. PERFORMING ORGANIZATION NAME(S) AND ADDRESS(ES)</b> Trustees of Boston College Institute for Space Research 140 Commonwealth Avenue Chestnut Hill, MA 02167			<b>8. PERFORMING ORGANIZATION REPORT NUMBER</b>	
<b>9. SPONSORING/MONITORING AGENCY NAME(S) AND ADDRESS(ES)</b> Phillips Laboratory Hanscom AFB, MA 01731-5000 Contract Manager: R. O'Neil/GPOS			<b>10. SPONSORING/MONITORING AGENCY REPORT NUMBER</b> PL-TR-92-2249	
<b>11. SUPPLEMENTARY NOTES</b>				
<b>12a. DISTRIBUTION/AVAILABILITY STATEMENT</b>  Approved for public release; distribution unlimited			<b>12b. DISTRIBUTION CODE</b>	
<b>13. ABSTRACT (Maximum 200 words)</b>  Reported are predictions of spectrum signal and total system noise for the MSX SPIRIT III interferometer as a function of both line-of-sight tangent height and wavelength. Also given are estimates of the tangent heights corresponding to saturation of the electronics. These results provide a basis for the final section of the interferometer bands and for developing MSX earthlimb background experiment plans.				
<b>14. SUBJECT TERMS</b> MSX SPIRIT III Limb radiance profiles			<b>SHARC code</b> MODTRAN code signal-to-noise	
			<b>15. NUMBER OF PAGES</b> 36	
			<b>16. PRICE CODE</b>	
<b>17. SECURITY CLASSIFICATION OF REPORT</b> UNCLASSIFIED	<b>18. SECURITY CLASSIFICATION OF THIS PAGE</b> UNCLASSIFIED	<b>19. SECURITY CLASSIFICATION OF ABSTRACT</b> UNCLASSIFIED	<b>20. LIMITATION OF ABSTRACT</b> SAR	

## CONTENTS

INTRODUCTION . . . . .	1
COMPONENTS OF THE TOTAL SYSTEM NOISE . . . . .	4
3-D REPRESENTATION OF NOISE AND SIGNAL . . . . .	6
INTERFEROMETER PERFORMANCE FOR TANGENT HEIGHTS 64 TO 110 KM . . . . .	8
INTERFEROMETER PERFORMANCE ABOVE 100 KM AND BELOW 64 KM . . . . .	16
SUMMARY . . . . .	23

## APPENDICES

A. PARAMETER VALUES USED IN THE SPIRIT III INTERFEROMETER MODEL . . . . .	27
B. LIST OF ACRONYMS . . . . .	29

DTIC QUALITY INSPECTED 1

<b>Accession For</b>	
NTIS GRA&I	<input checked="" type="checkbox"/>
DTIC TAB	<input type="checkbox"/>
Unannounced	<input type="checkbox"/>
Justification	
By _____	
Distribution/	
Availability Codes	
Dist	Avail and/or Special
A-1	

## PREFACE

The work described herein was performed for the Boston College Institute for Space Research under Subcontract No. 956-2, in support of prime Contract F19628-91-K-0001. The author wishes to thank the following individuals for providing valuable guidance, data or helpful discussions: Drs. Robert O'Neil and Harold Gardiner of Phillips Laboratory/GPO, Dr. A. T. Stair Jr. of ATSA, and Dr. Clair Wyatt of the Space Dynamics Laboratory at Utah State University.

# PERFORMANCE PREDICTIONS FOR THE MSX SPIRIT III INTERFEROMETER SPECTROMETER

## INTRODUCTION

The purpose of this interim technical report is twofold: to provide a basis for making the final selection of the six SPIRIT III interferometer spectral channels, and to provide preliminary estimates of expected interferometer performance for use by the Earthlimb Backgrounds Team in planning experiments for MSX.

There are at present seven interferometer channels if the recently proposed 2.6-4.9  $\mu\text{m}$  channel is included in the count. The interferometer focal plane will accommodate only six detectors/filters and therefore one of the seven channels will have to be eliminated. The filter for channel 2 originally covered the band 4.23-7 $\mu\text{m}$ ; a replacement filter, extending from 4.2 to 7  $\mu\text{m}$ , has been ordered by SDL so that channel 2 will provide spectrally resolved data over the full range of the SPIRIT III radiometer filters B1 (4.2-4.36) and B2 (4.2-4.45  $\mu\text{m}$ ). The table below lists the seven interferometer (IFR) channels; note that ?? is the designation used here for the proposed 2.6-4.9  $\mu\text{m}$  channel. Figure 1 shows the object-space projection of the present focal plane, with its six detector/filter channels; the projection is as seen by an observer looking in the same direction as the interferometer.

**SPIRIT III IFR CHANNELS**

Channel	Wavelength range( $\mu\text{m}$ )
4(OOPEN)	4.05-29
6(PREW)	4.9-29
2	4.2-7
??	2.6-4.9
3	5.8-8.9
1	17-26
5	10.5-13

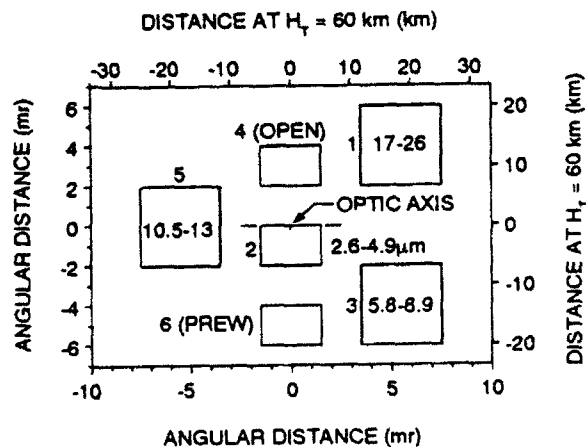


Fig. 1. Focal plane (object-space projection).

Figure 2 compares the wavelength coverage of the interferometer and radiometer bands. Figures 3 and 4 indicate some of the more important species in the quiescent and aurorally-disturbed atmosphere and show their locations relative to the IFR bands. The two quiescent spectra are predictions by SHARC for the nighttime subarctic atmosphere for a line-of-sight tangent height of 100 km; the auroral enhancements are predictions by the SHARC-2 code for an IBC III aurora seen at 100 km. Note that SHARC (and the spectrum shown in Fig. 3) does not include all of the species labeled in Fig. 3.

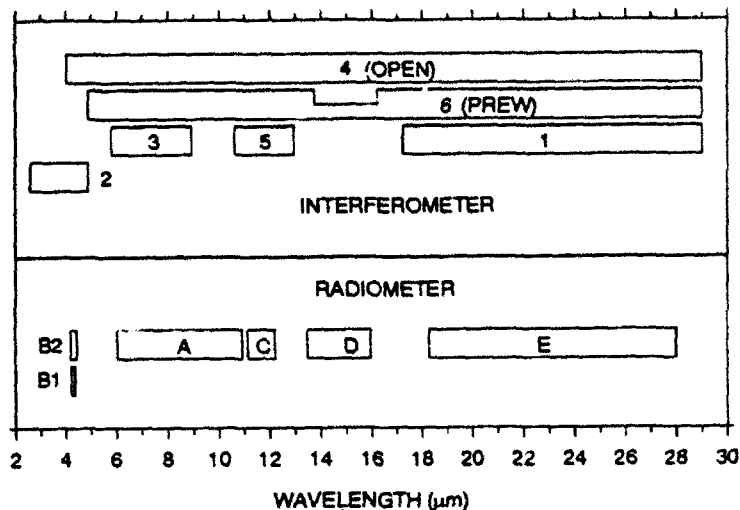


Fig. 2. SPIRIT III interferometer and radiometer bands.

The results given in this report consist primarily of predictions of spectrum signal and total system noise, as a function of both line-of-sight tangent height and wavelength across each IFR channel, and the tangent heights corresponding to saturation (interferogram clipping). The results are presented in a form that makes it easy to compare the implied S/N performance of different channels at the same tangent height and wavelength. Included in the Summary section is a table giving the useful tangent height range for each channel based on the implied S/N's and computed clipping altitudes.

The following two sections give a brief, qualitative description of the total system noise and the dependence of noise on signal, and explain the format of the three-dimensional figures used to characterize the IFR performance. This is followed by a section that presents the 3-D performance results for the tangent height range 64-100 km and a section that gives similar predictions for tangent heights above and below this range. The final section consists of a summary table and a series of figures showing the effective band photon radiance versus tangent height for each channel.

The predictions given herein are based on a computer code developed by ARC and on a simple model of the SPIRIT III interferometer. The model was recently upgraded to use new detector quantum efficiencies provided by SDL; however, the ones in the present model may not be representative of the latest measurements. The model uses assumed optical efficiencies and an assumed modulation index rather than values based on measurements that may now be available. Thus, while the resulting performance predictions may differ from actual performance, they should be sufficiently accurate for the purposes stated above. Appendix A lists all of the parameter values of the model that affect the predicted noise values. It is anticipated that the present model will be updated as more engineering data becomes available from SDL, and that some of the performance results will be recomputed. A future report may present the revised results. Appendix B lists the acronyms used in this report.

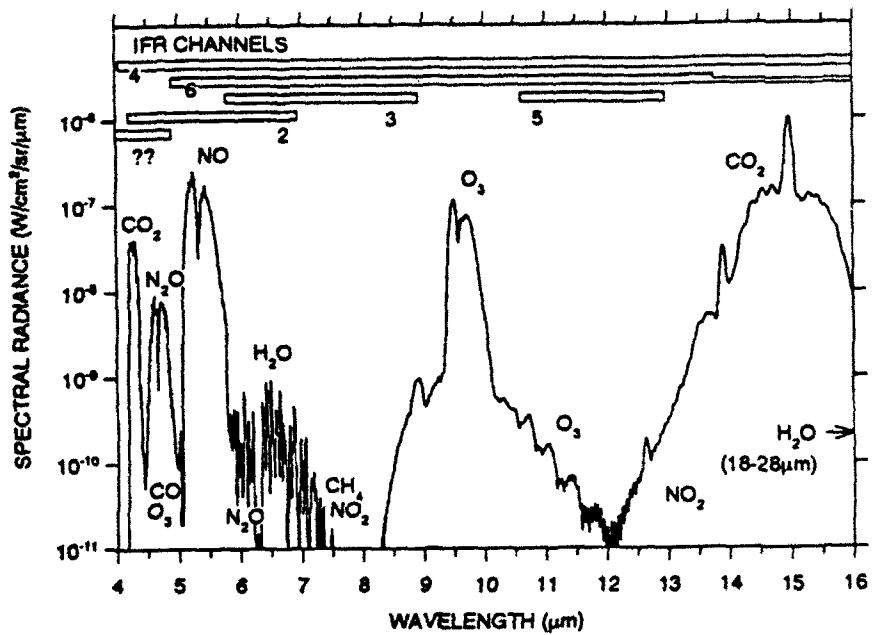


Fig. 3. Species observable in the interferometer channels (quiescent atmosphere).

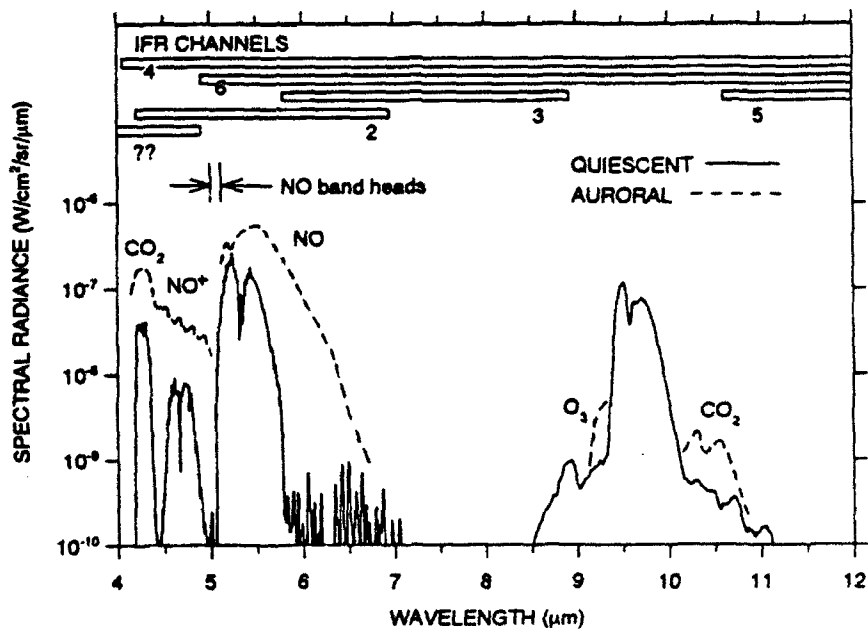


Fig. 4. Species observable in the interferometer channels (auroral enhancements).

## COMPONENTS OF THE TOTAL SYSTEM NOISE

The primary sources of noise are

- Preamp-Johnson noise (dark noise or NESR)
- Photon noise, and
- Digitization noise due to A/D conversion

MOSFET noise will likely be present at some frequencies, but is not included in the present analysis.

The noise-equivalent spectral radiance (NESR) is independent of input signal whereas the photon noise increases in proportion to the square root of the effective photon radiance in the interferometer filter band, as illustrated in Fig. 5. The effective band photon radiance (BPR) is defined as the photon spectral radiance at the entrance aperture times a wavelength-dependent detector quantum efficiency integrated over the filter band.

The A/D noise increases with BPR in a step-wise fashion with each factor-of-two reduction in gain. The gain can be switched (increased or decreased) up to six times. The BPR level at which the gain is switched depends on whether the BPR is increasing or decreasing. Hence, there are "hysteresis loops", or equivalently, two possible gain states (two levels of A/D noise) over a wide range of BPR levels. The interferogram central fringes may eventually become clipped if the BPR continues to increase beyond the level corresponding to the sixth gain change.

Figure 6 shows the total system noise, which is the root-sum-square of the three noise components. Figures 5 and 6 are shown primarily to indicate the qualitative nature of the variation of total noise with BPR. However, the figures apply quantitatively to a particular interferometer channel and a particular wavelength within the channel, as indicated. The noise plotted in these figures is output noise (eg, rms volts in the interferogram) equated to spectral radiance at the entrance aperture; it is the uncertainty in measured spectral radiance. In these units the noise depends on spectral resolution, ie, on interferogram length and any reduction in resolution resulting from apodization. Throughout this report noise values will always correspond to  $6 \text{ cm}^{-1}$  resolution, which implies the maximum-length SPIRIT III interferogram ( $2 \text{ cm}^{-1}$  resolution) apodized by a function that degrades the resolution by a factor of three.

Note that photon noise in this example is significant over a rather narrow range of BPR; it is never the dominant component of the total noise. This is typical of all channels of the SPIRIT III interferometer system, which uses a 12-bit A/D converter.

If a particular interferometer channel, model atmosphere and radiative transport code are specified, then the transport code can be used to compute a set of BPR values that are associated with line-of-sight tangent altitude, or LOSTA values: *Figures 5 and 6 could be replotted to show noise versus LOSTA and/or zenith angle.* The terms "tangent height" and LOSTA are used interchangeably throughout this report.

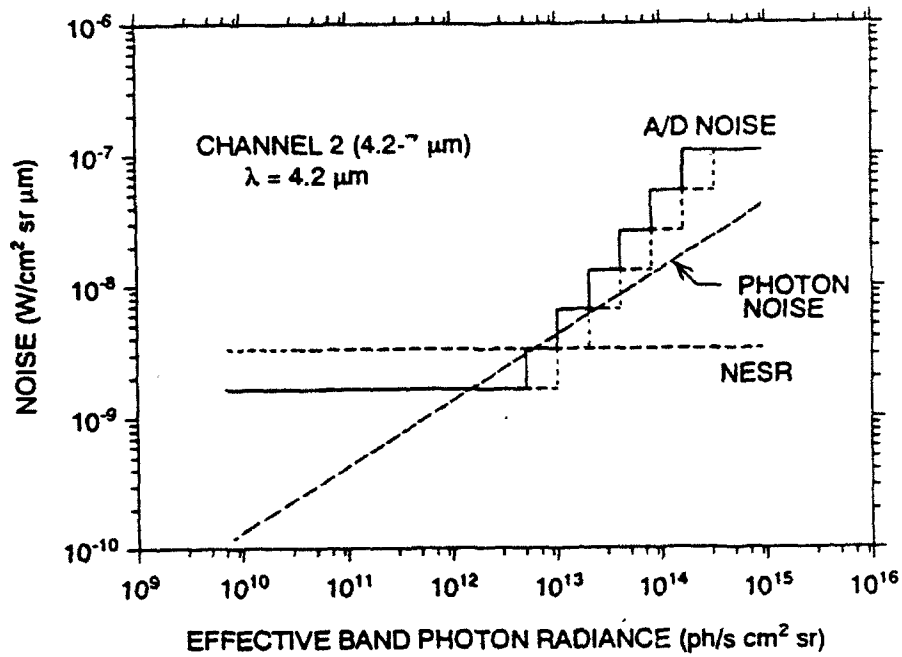


Fig. 5. The three components of total noise.

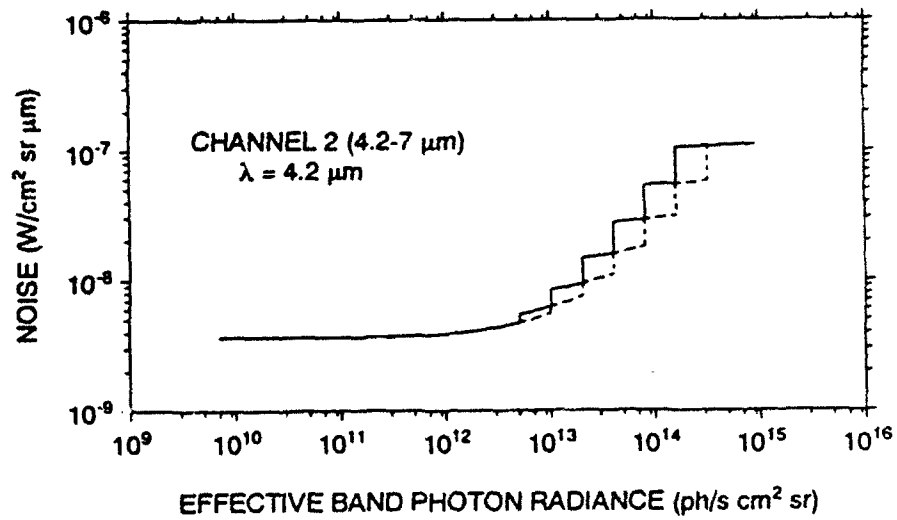


Fig. 6. The total noise versus effective band photon radiance.

### 3-D REPRESENTATION OF NOISE AND SIGNAL

Figure 7 shows the total noise plotted in the manner just described, except that the variation with wavelength  $\lambda$  is included: noise is displayed as a function of both LOSTA (denoted  $H_T$  in the figure) and wavelength. The figure corresponds quantitatively to the following specifics:

- Interferometer channel 4 (the OPEN channel), extending from 4.05 to 29  $\mu\text{m}$ ,
- Limb spectral radiances computed by the SHARC code for
- the nighttime subarctic summer model in SHARC, and
- 6  $\text{cm}^{-1}$  spectral resolution

Note that the interferogram for this case is clipped for tangent heights lower than approximately 63 km and that there are five gain changes between 110 and 63 km tangent height; hence, another gain change must occur above 110 km. The total noise displayed in the figure corresponds to the low-noise (high-gain) side of the gain hysteresis loops. All subsequent figures follow this convention. The noise is a minimum near wavelength 25  $\mu\text{m}$  where the detector has maximum responsivity.

Figure 8 is similar except that both signal and noise are displayed. The "signal" is the limb spectral radiance predicted by SHARC for the nighttime subarctic summer model degraded to 6  $\text{cm}^{-1}$  resolution (via simulation of the corresponding interferogram and subsequent Kaiser-Bessel apodization with  $\alpha = 3$ ). As indicated, the signal is shown only for selected tangent heights. *This is an example of the many signal and noise (S,N) plots to follow.* They allow a quick visual assessment of approximate signal-to-noise ratio versus tangent height and/or below-the-horizon (BTH) zenith angle, for the major atmospheric molecular bands and windows regions. All figures correspond to the subarctic summer atmosphere, either night or day, as indicated in the figure title. Spectral radiances for tangent heights of 60 km and greater were computed using the current version of SHARC; the MODTRAN code was used for  $H_T \leq 50$  km and for BTH.

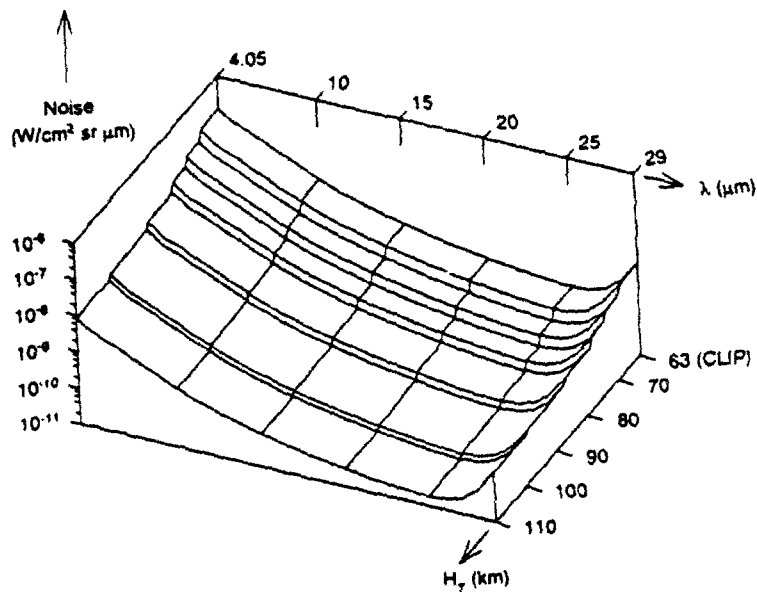


Fig. 7. Interferometer total noise vs. wavelength and tangent height; for SHARC/NIGHT and channel 4 (OPEN), which covers 4.05 to 29 μm.

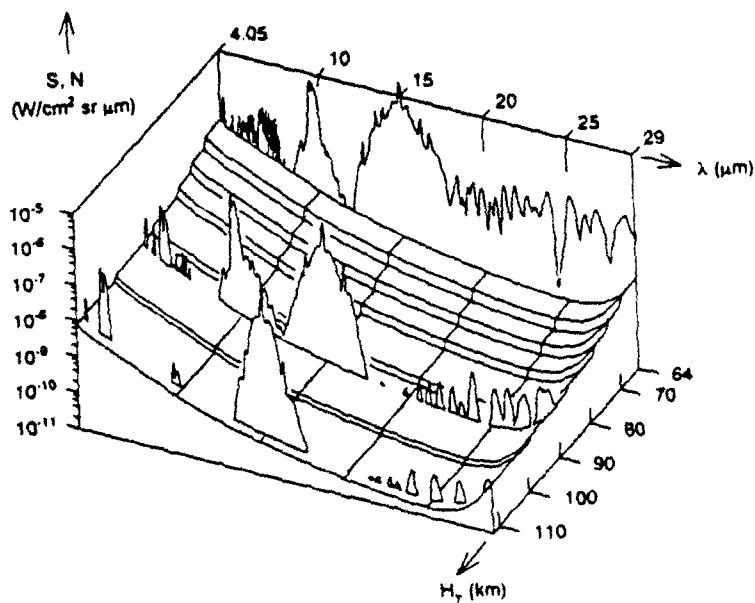


Fig. 8. Same as Fig. 7 except that signal is also displayed. The signal S is shown for the LOSTAs 64, 90 and 110 km.; the interferogram is clipped at 63 km.

## INTERFEROMETER PERFORMANCE FOR TANGENT HEIGHTS 64 TO 110 KM

The series of figures in this section show the performance of the SPIRIT III interferometer for all seven channels over the tangent height range 64 to 110 km. The axis defining tangent height  $H_T$  and the log scale showing signal  $S$  and noise  $N$  are essentially the same in all figures, which facilitates the comparison of performance for channels with overlapping filter bands. Figure 9 shows  $S$  and  $N$  for channel 1. Corresponding results for channels 4, 6, 2, ??, 3 and 5 are shown in Figs. 10 through 15.

The tangent height at which the interferogram becomes clipped is indicated in each figure. Clipping occurs at approximately 65 km for channel 1; Fig. 9 is the only one in the series for which the  $H_T$  scale starts above 64 km.

Channel 6 has a prewhitening filter, ie, a filter that over part of its spectral range (the "notch" region) has greatly reduced transmission so as to whiten, or make more uniform, the spectral distribution of photon flux reaching the detector. Hence, the figure for channel 6 (Fig. 11) shows a region of elevated total noise in the notch region, approximately 13.7 and 16.1  $\mu\text{m}$  wavelength. The noise, in fact, is 100 times greater than at wavelengths outside the notch since the transmittance value used for the notch region is 0.01. Note that channel 6 gives approximately three times higher  $S/N$  than channel 4 (the Open channel) in the 5.3  $\mu\text{m}$   $\text{NO}$  and 9.6  $\mu\text{m}$   $\text{O}_3$  bands at  $H_T = 110$  km. The reduction in band photon flux (BPR) effected by the prewhitening results in both slightly reduced photon noise and a factor-of-two reduction in A/D noise; ie, the gain at 110 km is one level higher for channel 6 than for channel 4, as can be seen in Figs. 11 and 10. Widening the prewhitening notch would not significantly improve performance at 110 km because the photon noise is already a small portion of the total noise and because the gain is at its highest level.

Channel ?? has been proposed to view low tangent heights and BTH scenes. Similarly, channel 2 can obtain data down to 8 km without clipping. Hence, the figures for these channels (Figs. 13 and 12) are not representative of their performance. The next section gives  $S,N$  figures for tangent heights greater than 110 km and lower than 64 km.

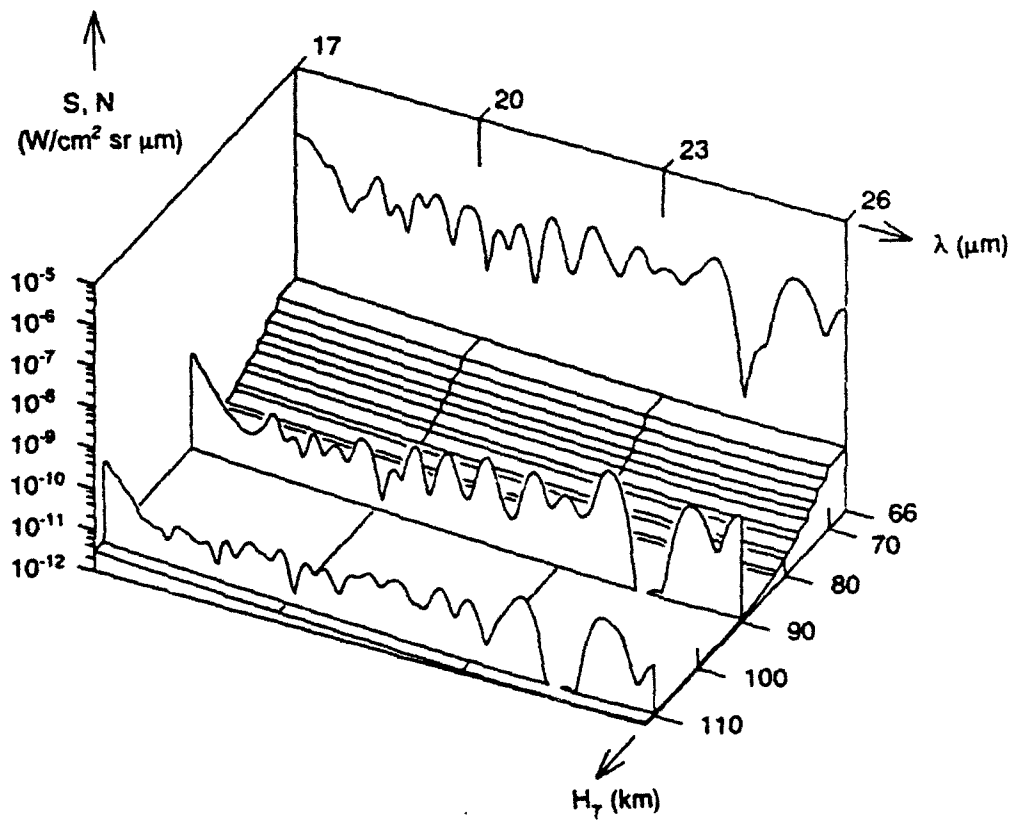


Fig. 9. S and N for channel 1 (17-26  $\mu m$ ); S is shown for 66, 90 and 110 km. The interferogram is clipped at 65 km.

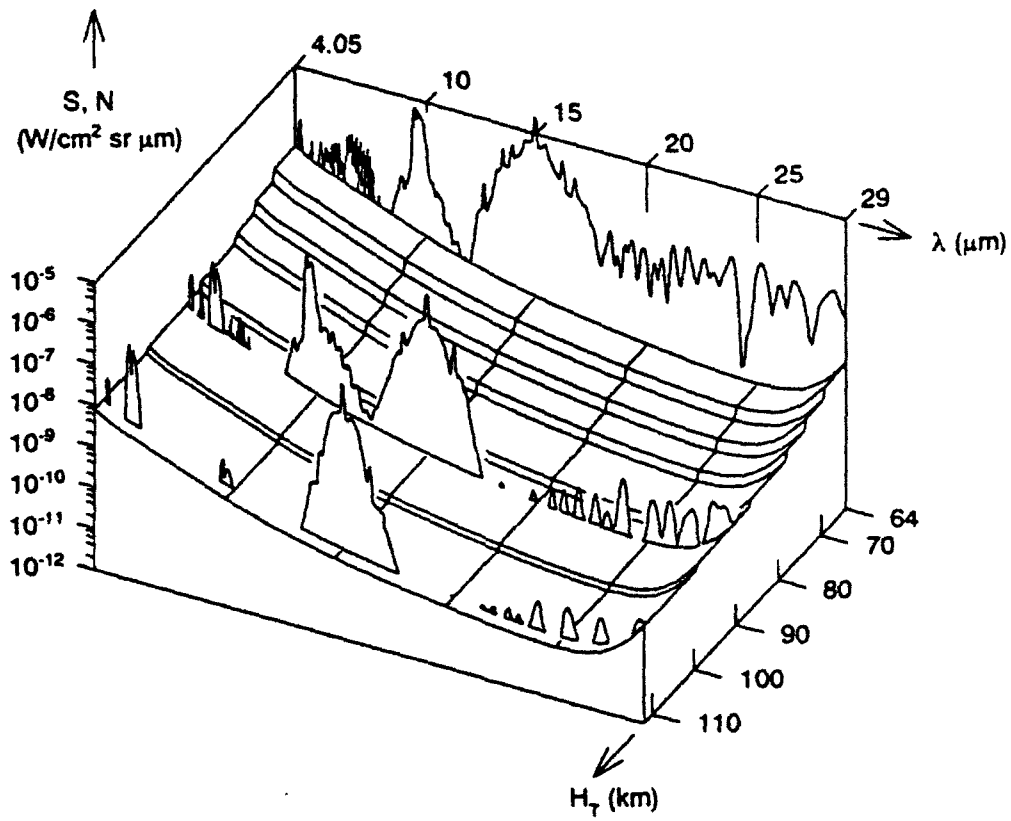


Fig. 10. S and N for channel 4 (4.05-29  $\mu m$ ); S is shown for 64, 90 and 110 km. The interferogram is clipped at 63 km.

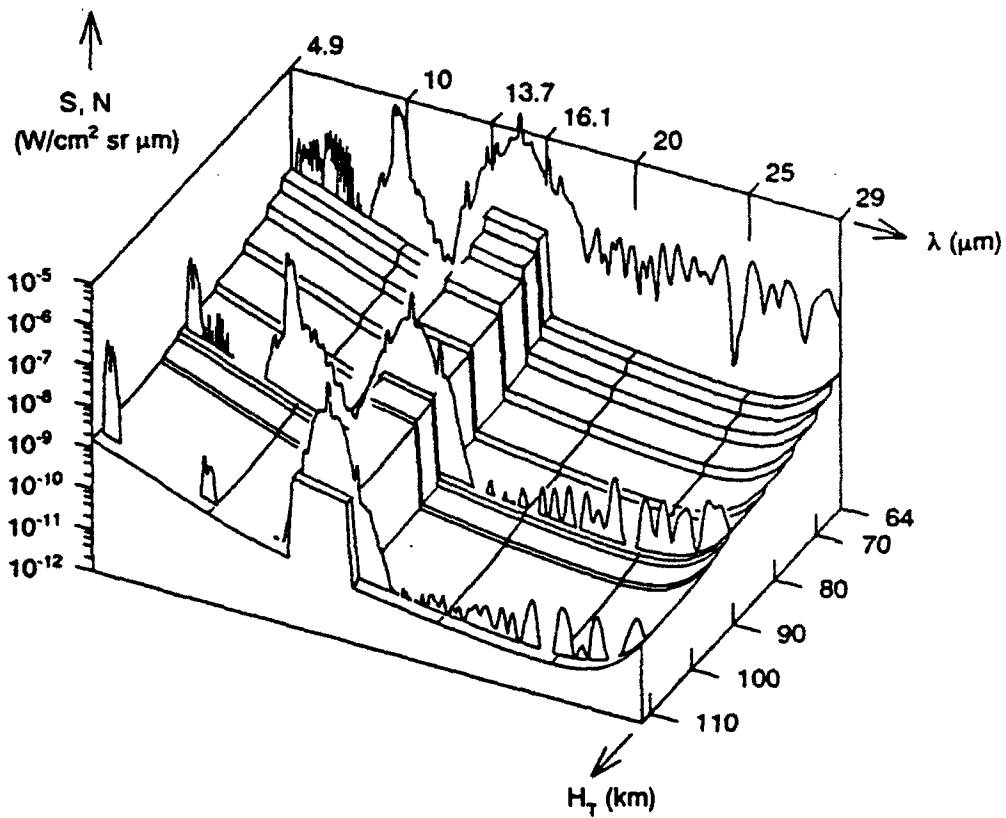


Fig. 11. S and N for channel 6 (4.9-29  $\mu m$ ); S is shown for 64, 90 and 110 km. The interferogram is clipped at 61 km.

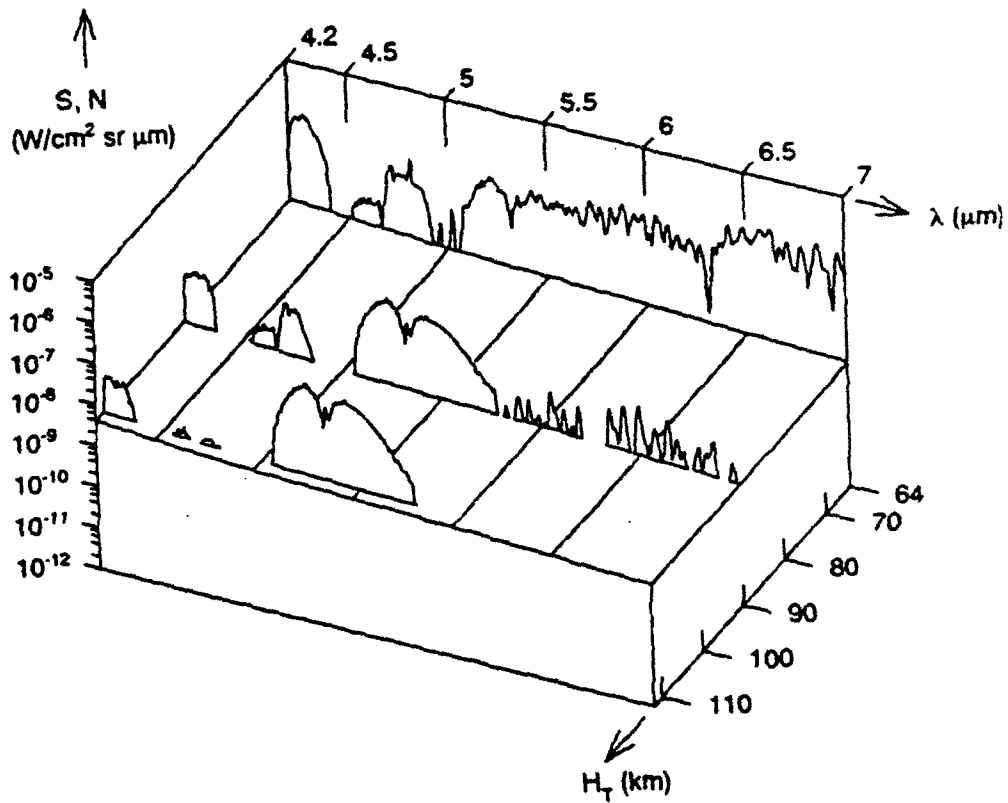


Fig. 12. S and N for channel 2 (4.2-7  $\mu m$ ); S is shown for 64, 90 and 110 km. The interferogram is clipped at 8 km.

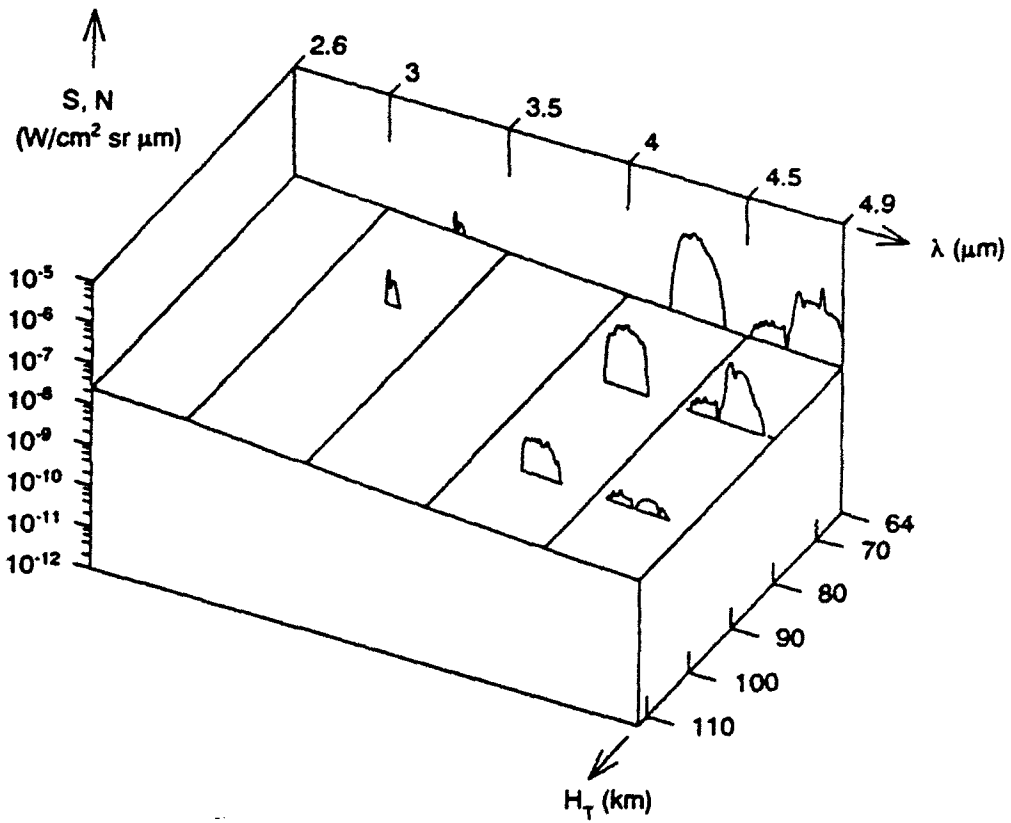


Fig. 13. S and N for channel ?? (2.6-4.9  $\mu m$ ); S is shown for 64, 80 and 100 km. The interferogram is not clipped either ATH or BTH.

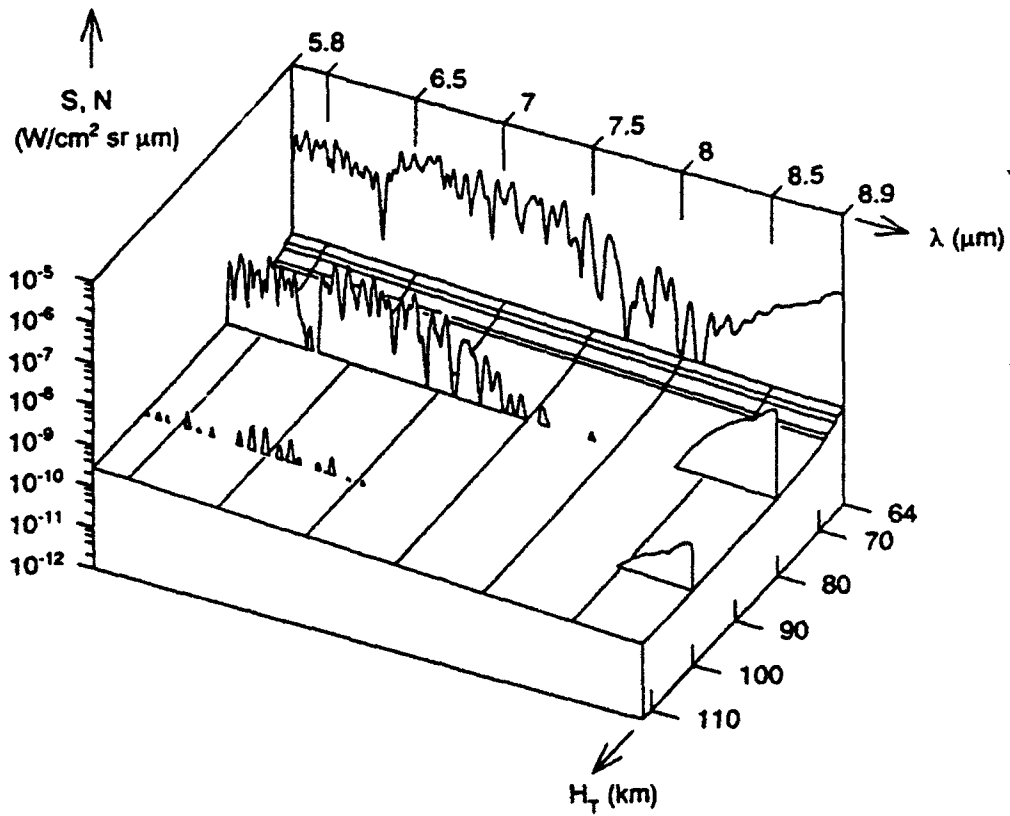


Fig. 14. S and N for channel 3 (5.8-8.9  $\mu\text{m}$ ); S is shown for 64, 80 and 110 km. The interferogram is clipped at 49 km.

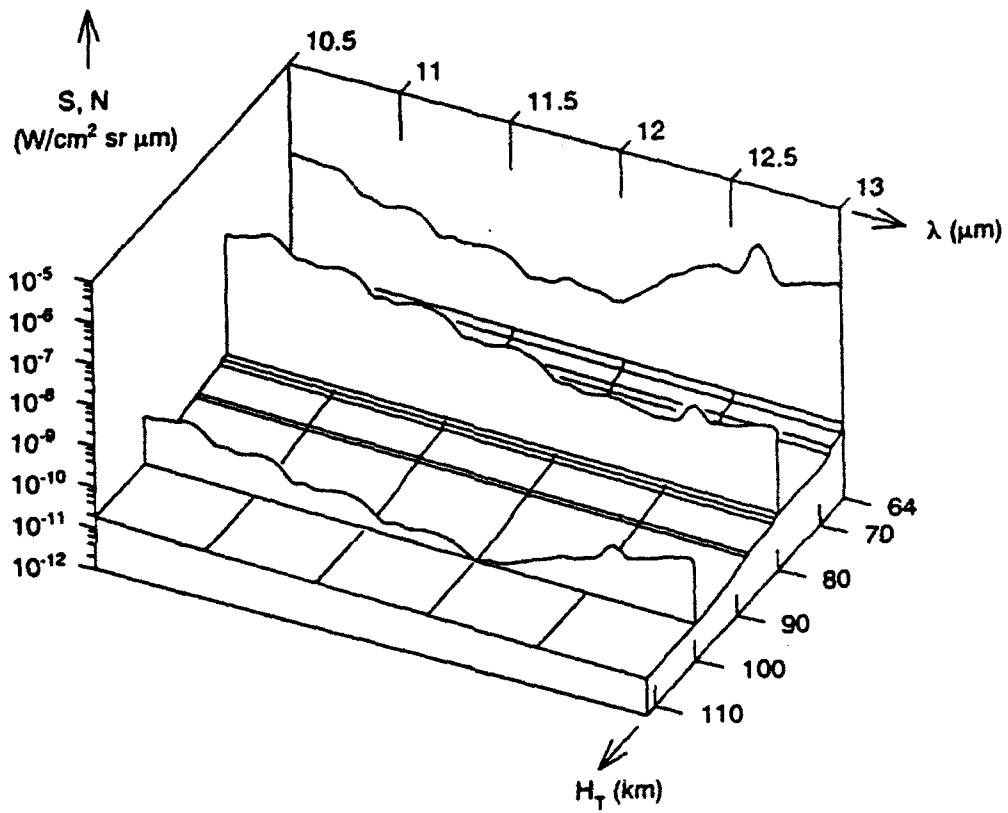


Fig. 15. S and N for channel 5 (10.5-13  $\mu\text{m}$ ); S is shown for 64, 80 and 110 km. The interferogram is clipped at 55 km.

## INTERFEROMETER PERFORMANCE ABOVE 100 KM AND BELOW 64 KM

This section extends the S,N figures of the previous sections to higher and/or lower tangent heights, as appropriate for each interferometer channel. The first three figures (16 through 18) correspond to channels 1, 4 and 6, and show S and N from  $H_T = 90$  km up to the tangent height at which the maximum S/N in the spectrum is approximately 10; these  $H_T$ 's are 210, 180 and 180 km, respectively. There are no corresponding figures for  $H_T$  less than 64 km for channels 1, 4 and 6; they clip at 65, 63 and 61 km.

Following these are two figures for channel 2 (4.2-7  $\mu$ m). Figure 19 covers the tangent height range 100 to 180 km; Fig. 20 covers 10 to 100 km.

The section continues with more text and Fig. 21, which describe the performance of channel ???. This channel does not clip even when viewing the nadir, and has adequate S/N (in the 4.3  $\mu$ m  $\text{CO}_2$  band) up to  $H_T = 100$  km.

There is no figure in this section for channel 3 since it has maximum S/N  $\approx 10$  at  $H_T = 100$  km and is clipped at 46 km; Fig. 14 in the last section adequately defines its performance. The present section ends with Fig. 22, which shows S and N for channel 5.

As pointed out earlier, the noise N and signal S both correspond to spectral radiances predicted by the SHARC or MODTRAN codes; SHARC/night is used for  $H_T > 50$  km and MODTRAN/day is used for  $H_T \leq 50$  km. In the MODTRAN/day case, the Earth albedo is 0.4 and the Sun is at zenith. Thus, the performance results given here tend to be conservative: the predicted S/N tends to be "low" at tangent heights above 50 km, and the predicted S tends to be "high" for  $H_T < 50$  and for BTH, which implies clipping at generally higher tangent heights or smaller BTH zenith angles.

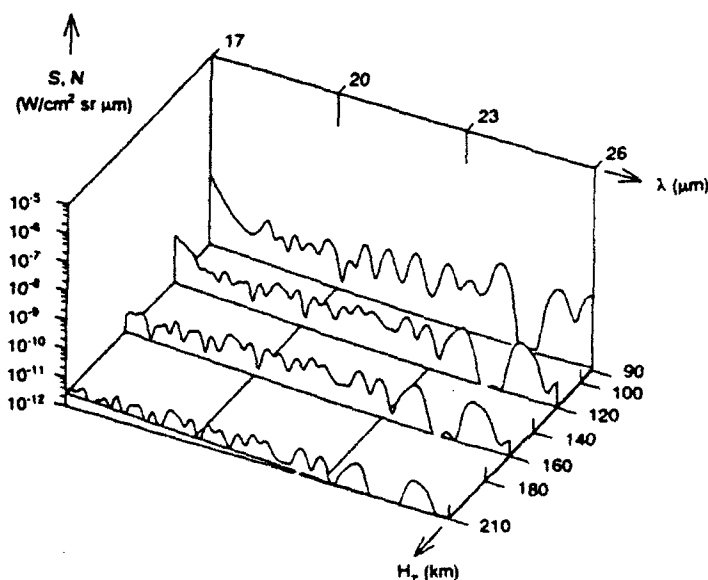


Fig. 16. S and N for channel 1 (17-26  $\mu$ m); S is shown at 90, 120, 160 and 210 km.

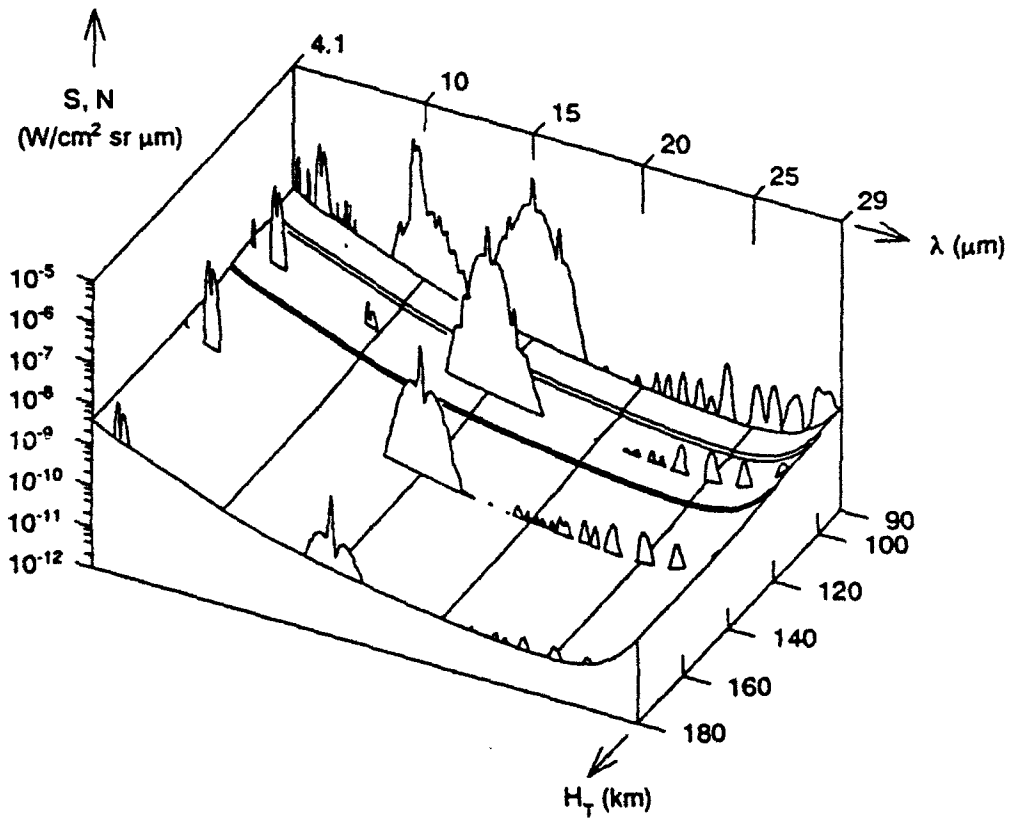


Fig. 17. S and N for channel 4 (4.05-29  $\mu m$ ); S is shown for 90, 110, 140 and 180 km.

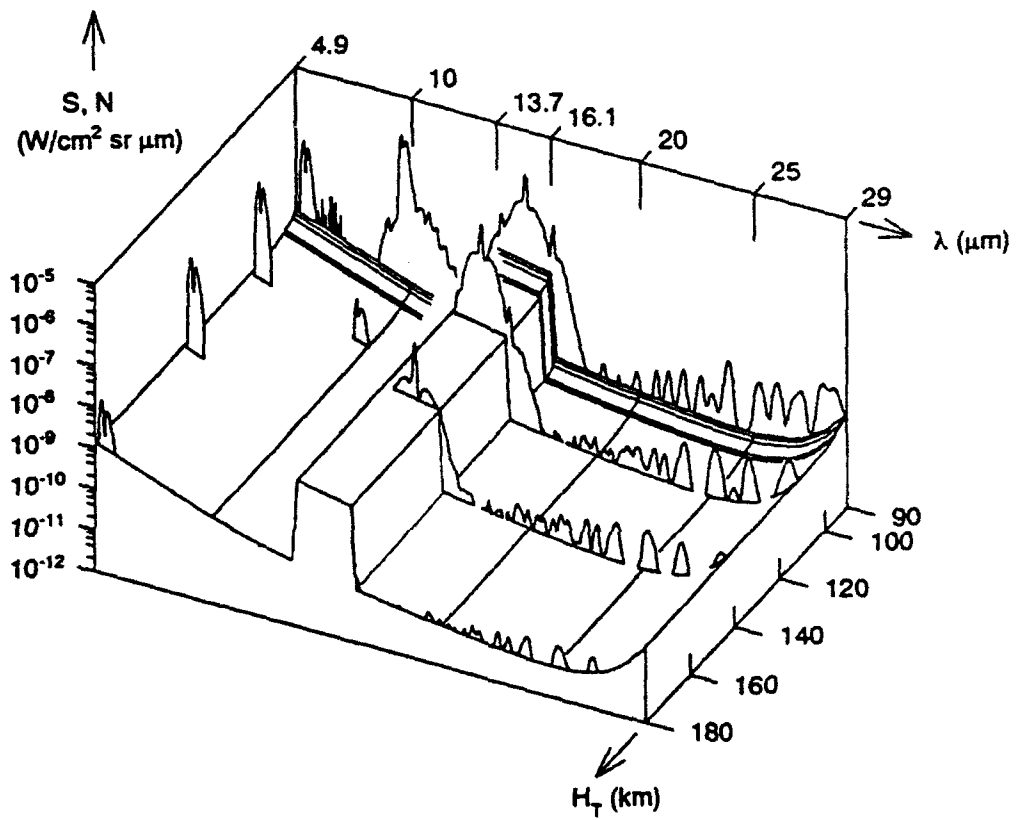


Fig. 18. S and N for channel 6 (4.9-29  $\mu m$ ); S is shown for 90, 110, 140 and 180 km.

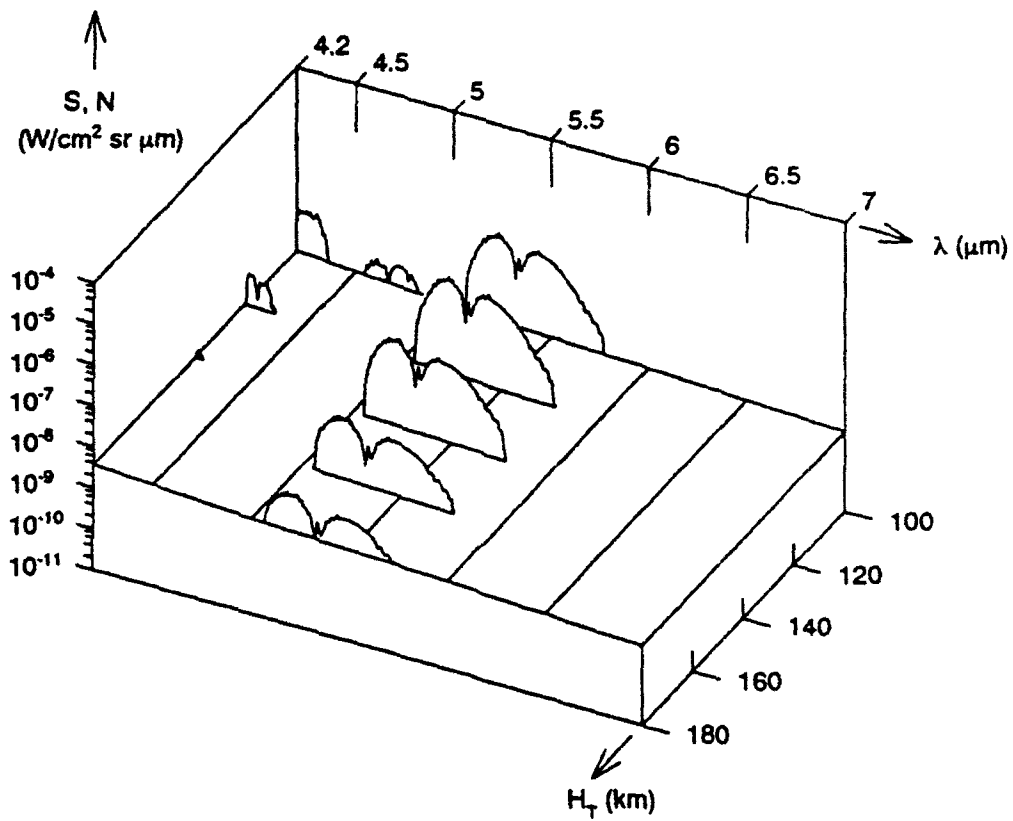


Fig. 19. S and N for channel 2 (4.2-7 μm); S is shown for 100, 120, 140, 160 and 180 km.

Figure 21 is the S,N plot for the proposed 2.6-4.9  $\mu\text{m}$  channel. Note that the axis representing the viewing direction gives the line-of-sight (LOS) zenith angle for BTH viewing directions, and gives tangent height when the LOS is ATH. The axis ranges from 180 degrees (nadir) to 110 km. The interferogram for channel ?? is not clipped even when the interferometer views the nadir. The hard horizon ( $H_T = 0$ ) occurs at approximately 118 degrees zenith angle; at this point viewing changes from BTH to ATH and, of course, the spectrum changes dramatically in character. The signal spectrum is shown for zenith angles of 180 and 118 degrees and for tangent heights of 20, 60 and 100 km.

Note that all seven gain levels are represented in the figure, and that the gain change down to the lowest gain level (highest A/D noise level) occurs midway between zenith angles 145 and 118 degrees, ie, at about 130 degrees. As shown in the next section, the BPR increases very slowly with zenith angle between 118 and 180 degrees; at nadir the BPR is still three times lower than the level that would result in clipping of the interferogram.

Figure 22 shows the S and N spectra for channel 5 over the LOSTA range 80 to 110 km.

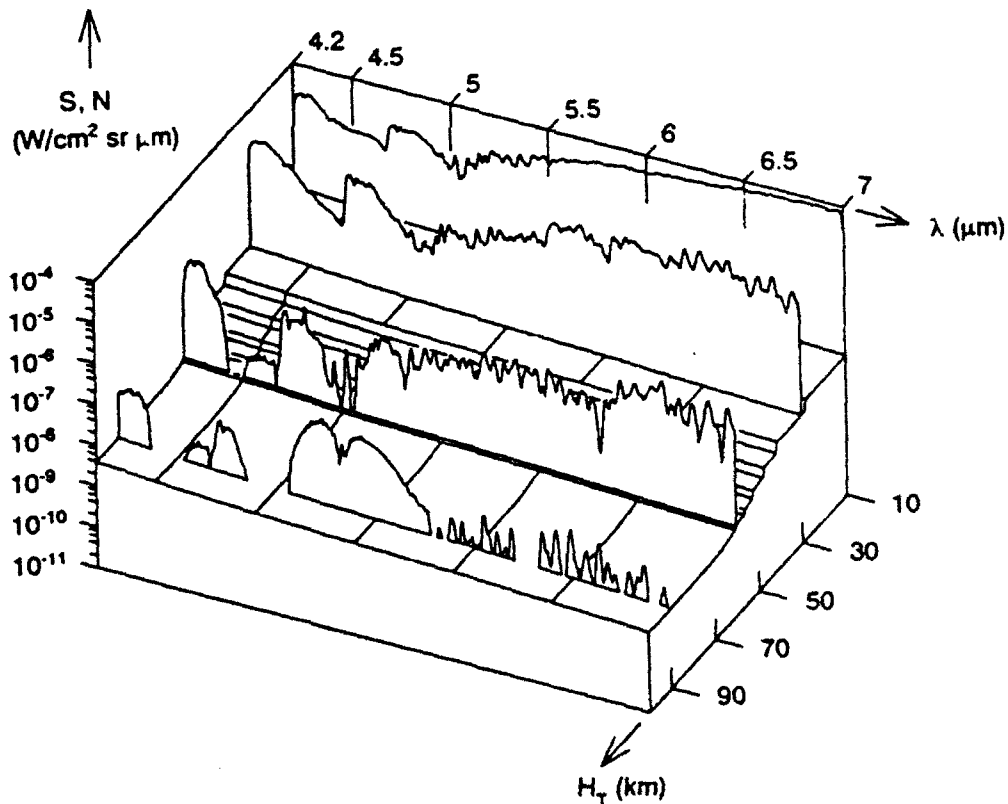


Fig. 20. S and N for channel 2 (4.2 -7  $\mu\text{m}$ ); S is shown for 10, 30, 60 and 90 km. The interferogram is clipped at 8 km.

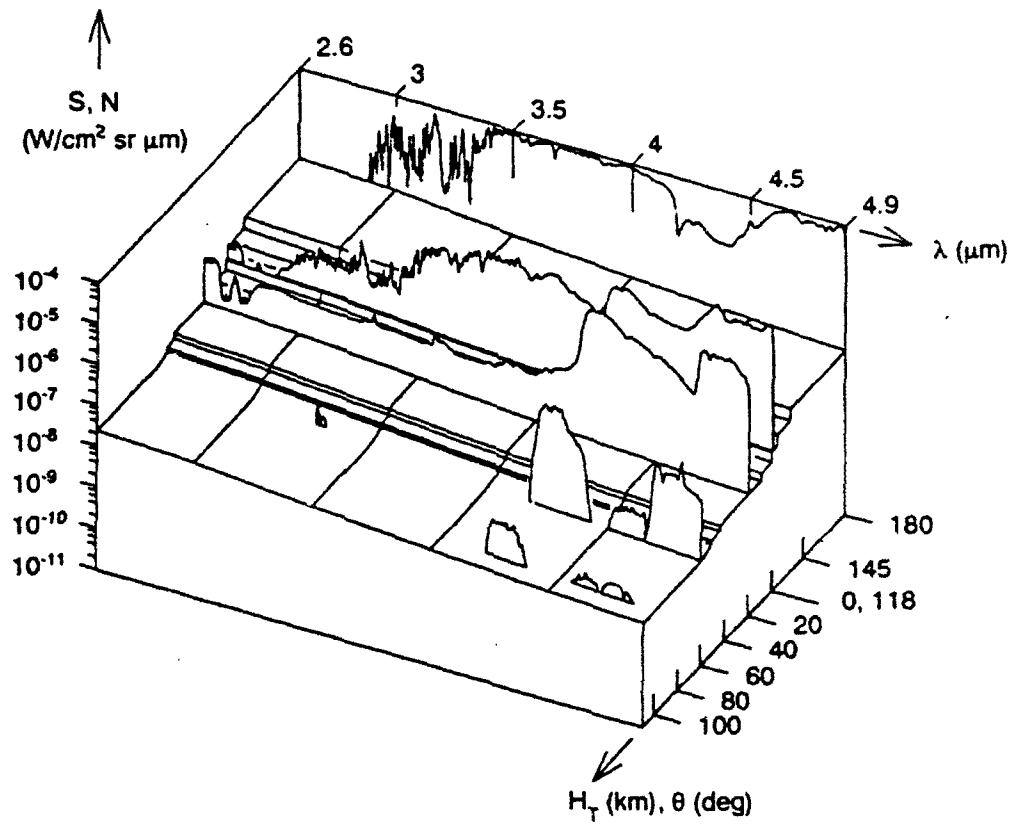


Fig. 21. S and N for channel ?? (2.6-4.9  $\mu m$ ); S is shown at 180 and 118 deg., and for 20, 60 and 100 km. The interferogram is not clipped.

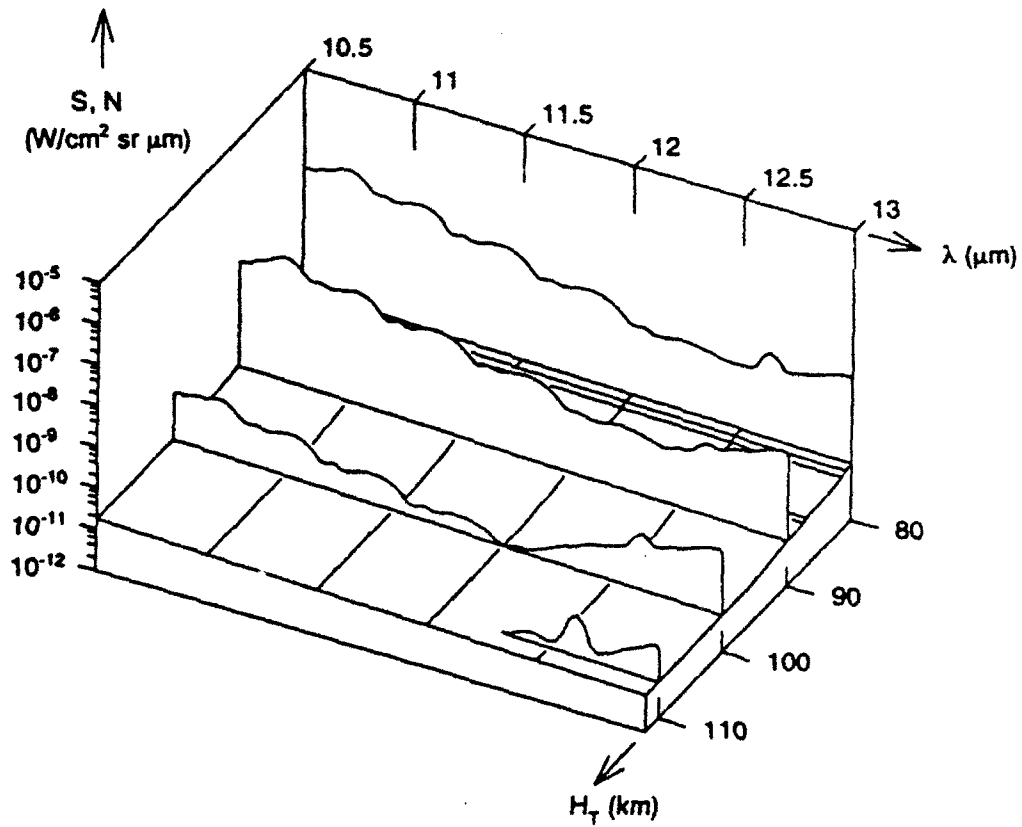


Fig. 22. S and N for channel 5 (10.5-13  $\mu\text{m}$ ); S is shown for 80, 90, 100 and 110 km.

## SUMMARY

Figures 23 through 25 show the effective band photon radiance (BPR) as a function of LOSTA. Each shows the BPR level that produces clipping in the interferogram. These figures provide a quick means of estimating the change in clipping LOSTA that would result from a "change" in instrument sensitivity. The sensitivity "change" could be the result of design changes made by SDL or the result of using updated values in our model of the SPIRIT III interferometer, eg, more accurate data on optical losses or quantum efficiencies. The LOSTAs at which clipping occurs determine the minimum altitudes for which species concentrations can be inferred from the interferometer data. The figures show the BPR for SHARC/day as well as SHARC/night even though the former are not used in the computation of total noise.

The table below lists, for each interferometer channel, the BPR clip level, the corresponding LOSTA, and the tangent height at which the maximum spectral radiance is ten times the noise. Listed also are the molecular species/bands that produce the signal corresponding to  $S/N = 10$ . The  $H_T$  pairs in the table represent the useful tangent height range of each interferometer channel.

Chan	Wavelength range( $\mu\text{m}$ )	$H_T(\text{km})$ for CLIP	$H_T(\text{km})$ for $S/N_{\text{max}}=10$	Species giving $S_{\text{max}}$	BPR* CLIP level
4(OPEN)	4.05-29	63	180	5.3 $\mu\text{m}$ NO, 15 $\mu\text{m}$ CO <sub>2</sub>	$1.1 \times 10^{15}$
6(PREW)	4.9-29	61	180	5.3 $\mu\text{m}$ NO	$5.2 \times 10^{14}$
2	4.2-7	8	180	5.3 $\mu\text{m}$ NO	$1.1 \times 10^{15}$
??	2.6-4.9	(NO CLIP)	100	4.3 $\mu\text{m}$ CO <sub>2</sub>	$2.0 \times 10^{15}$
3	5.8-8.9	49	100	9.6 $\mu\text{m}$ O <sub>3</sub> wing	$1.5 \times 10^{14}$
1	17-26	65	210	rot H <sub>2</sub> O	$6.0 \times 10^{13}$
5	10.5-13	55	110	15 $\mu\text{m}$ CO <sub>2</sub> wing	$6.0 \times 10^{13}$

\* Units are  $\text{ph/s cm}^2 \text{ sr}$ . BPR is the integral over the filter of the aperture photon radiance times the detector quantum efficiency. For channel 6 the photon spectral radiance is also multiplied by the transmittance (0.01) of the prewhitening filter over the prewhitened region. This allows a meaningful comparison of the BPRs for channels 6 and 4.

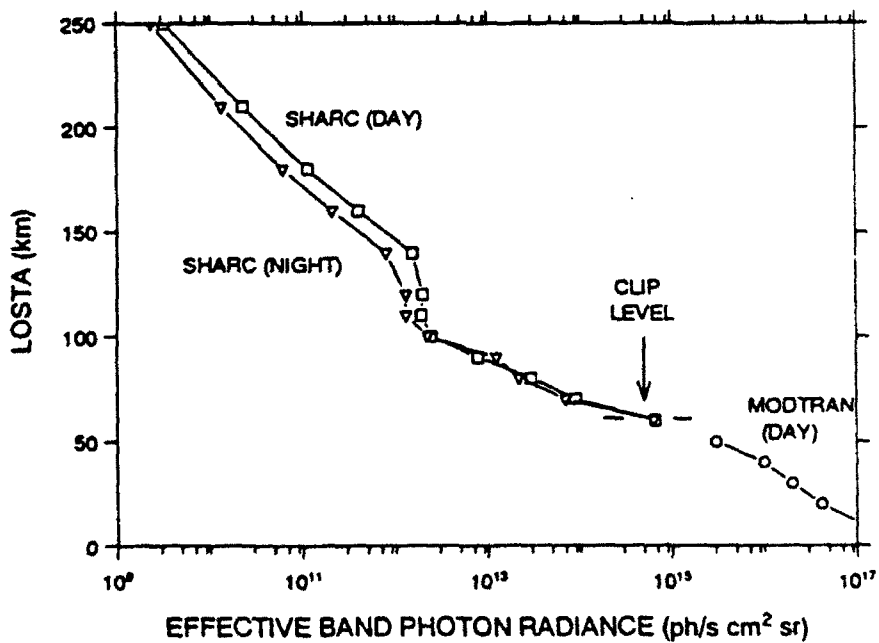
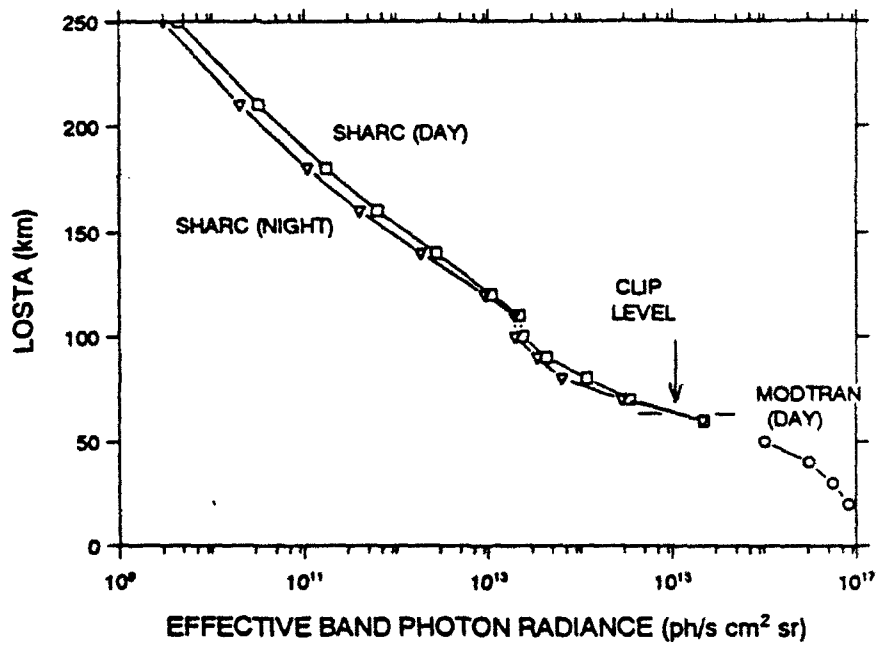


Fig. 23. Band photon radiance vs. LOSTA for channels 4 (top panel) and 6 (bottom).

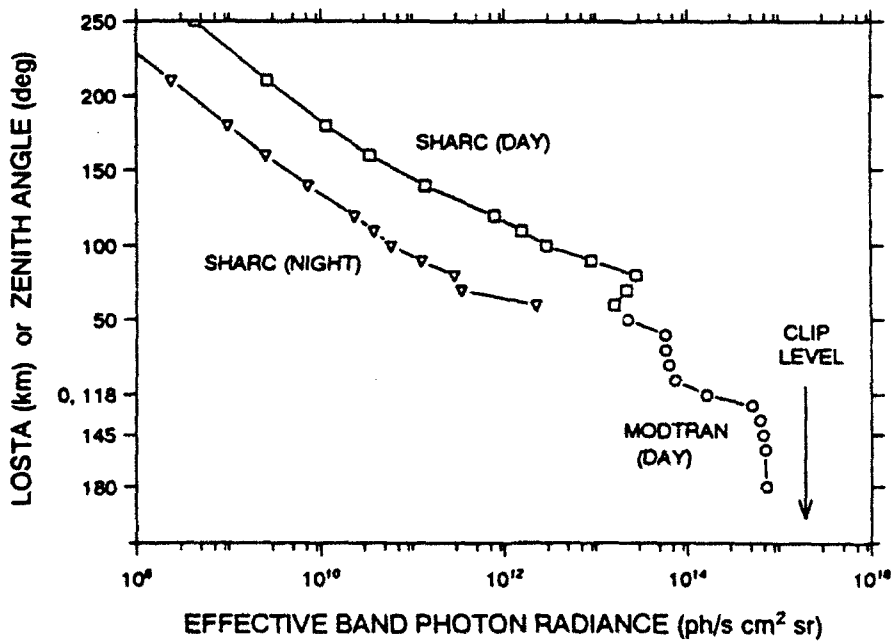
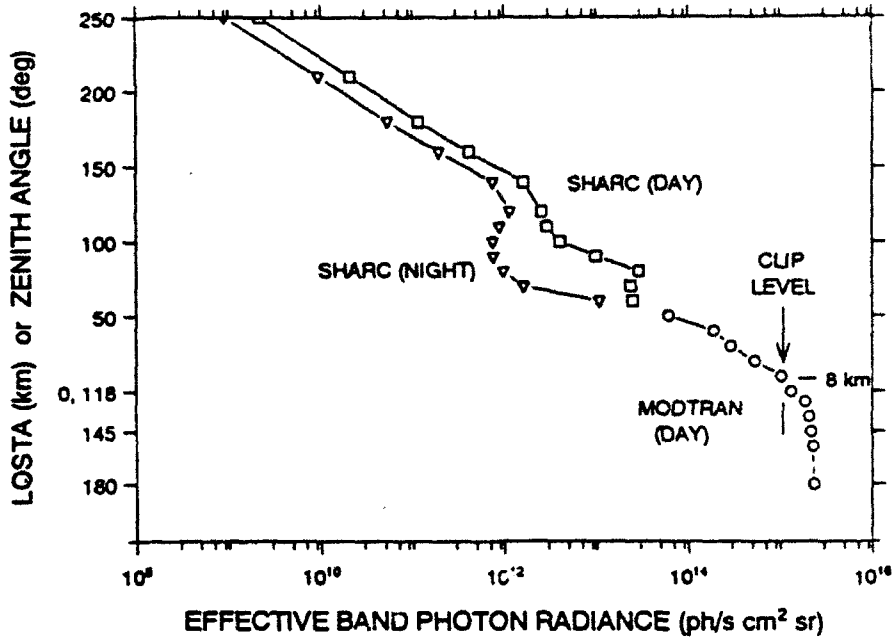


Fig. 24. Band photon radiance vs. LOSTA for channels 2 (top panel) and ?? (bottom).

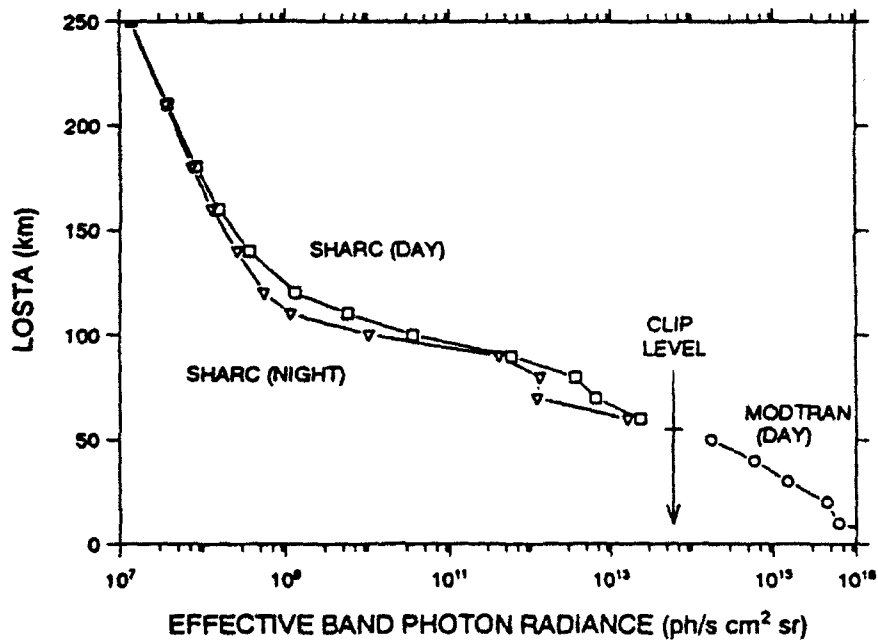
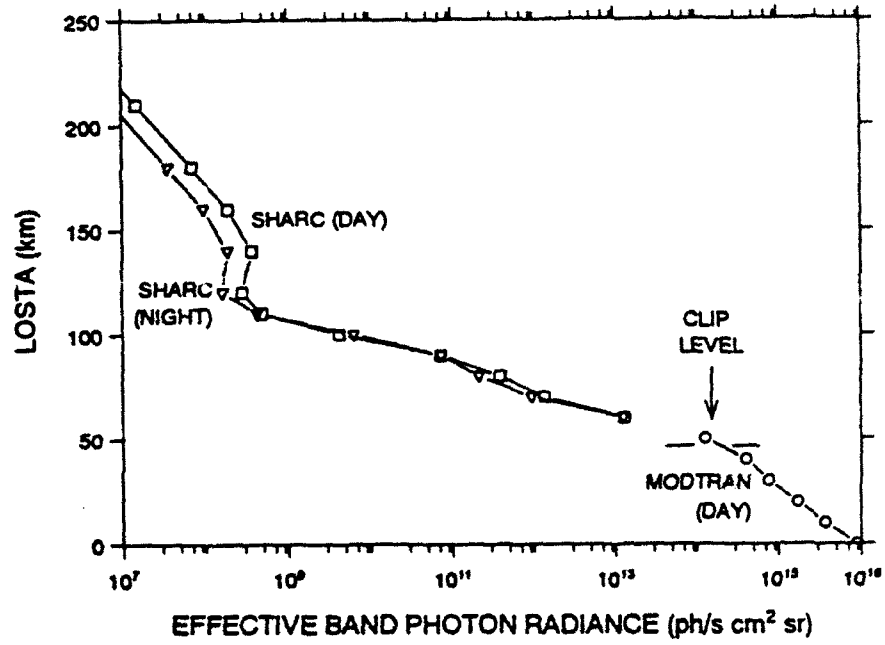


Fig. 25. Band photon radiance vs. LOSTA for channels 3 (top panel) and 5 (bottom).

## APPENDIX A

### PARAMETER VALUES USED IN THE SPIRIT III INTERFEROMETER MODEL

---

Large detector IFOV (channels 1, 3 and 5):	16.0 x 10 <sup>-6</sup> sr
Small detector IFOV (2, 4, 6 and ??):	6.0 x 10 <sup>-6</sup> sr
Collector area	393 cm <sup>2</sup>
Optical efficiency overall	0.122
Modulation index incl. in above efficiency	0.7
Transmission in reject notch of prewhitening filter	0.01

---

Voltage responsivity  $R = R_{20} \cdot (\lambda/20\mu\text{m}) \cdot (Q/Q_{20})$

Voltage responsivity at 20  $\mu\text{m}$   $R_{20} = 1.93 \times 10^9 \text{ V/W}$

Quantum efficiency at 20  $\mu\text{m}$   $Q_{20} = 0.897$

Quantum efficiency Q vs.  $\lambda$ :

$\lambda(\mu\text{m})$	Q	$\lambda$	Q	$\lambda$	Q
2.0	0.45	14.0	0.765	25.0	0.776
3.0	0.32	15.0	0.800	25.5	0.700
4.0	0.392	16.0	0.832	26.0	0.632
5.0	0.426	17.0	0.856	26.5	0.525
6.0	0.374	18.0	0.876	27.0	0.415
7.0	0.384	19.0	0.888	27.5	0.275
8.0	0.406	20.0	0.897	28.0	0.170
9.0	0.461	21.0	0.900	28.5	0.085
10.0	0.538	22.0	0.897	29.0	0.040
11.0	0.612	23.0	0.876	29.5	0.015
12.0	0.676	24.0	0.844	30.0	0.000
13.0	0.721				

TIA feedback resistance	$1.0 \times 10^8$ ohms
TIA input capacitance	$4.0 \times 10^{-11}$ farads
TIA input noise voltage	$1.0 \times 10^{-7}$ V
Detector/preamp operating temperature	10 K
<hr/>	
Information noise bandwidth (Hz):	
Channel 3 ( 5.8-8.9 $\mu\text{m}$ )	500
Channel 5 (10.5-13 $\mu\text{m}$ )	250
Channel 1 (17. -26 $\mu\text{m}$ )	250
Channel 6 ( 4.9-29 $\mu\text{m}$ )	600
Channel 2 ( 4.2-7.0 $\mu\text{m}$ )	1000
Channel ??( 2.6-4.9 $\mu\text{m}$ )	1500
Channel 4 (4.05-29 $\mu\text{m}$ )	1000
A/D full-scale input voltage	10 V
Number of A/D bits	12
DC level bits for gain reduction (gain $\rightarrow$ gain/2)	
DC level bits for gain increase (gain $\rightarrow$ gain/2)	
Max number of gain changes	6
<hr/>	
Number of interferogram sides	1
Unapodized resolutions	2, 5 and 20 $\text{cm}^{-1}$

## APPENDIX B

### LIST OF ACRONYMS

---

ATH	Above The Horizon
BPR	Band Photon Radiance
BTH	Below The Horizon
IFR	Interferometer
LOS	Line-Of-Sight
LOSTA	Line-Of-Sight Tangent Altitude
MSX	Midcourse Space Experiment
NESR	Noise Equivalent Spectral Radiance
PREW	Prewhitened channel in SPIRIT III
SDL	Space Dynamics Laboratory
SHARC	Strategic High Altitude Radiance Code
TIA	Transimpedance Amplifier